Nanoholes fabricated by self-assembled gallium nanodrill on GaAs(100)

Zh. M. Wang, B. L. Liang,[a] K. A. Sablon, and G. J. Salamo
Physics Department, University of Arkansas, Fayetteville, Arkansas 72701

(Received 6 December 2006; accepted 9 February 2007; published online 15 March 2007)

Self-assembled nanodrill technology based on droplet epitaxy growth was developed to obtain nanoholes on a GaAs(100) surface. In this technology, the gallium droplets act like "electrochemical drills" etching away the GaAs substrate beneath to give rise to nanoholes more than 10 nm deep. The driving force of the nanodrill is attributed to the arsenic desorption underneath the gallium droplet at high growth temperatures and Ga-rich condition. This nanodrill technology provides an easy and flexible method to fabricate nanohole templates on GaAs(100) surface and has great potential for developing quantum dots and quantum dot molecules for quantum computation applications. © *2007 American Institute of Physics*. [DOI: 10.1063/1.2713745]

There have been enormous worldwide research efforts in semiconductor nanostructures in the last decade. The basic motivation behind the study of semiconductor nanostructures is that the quantum-confinement effect in such low-dimensional systems allows devices with promising properties to be engineered.[1–6] As an example, an intriguing challenge that is now being explored is the possibility of using the quantum dot (QD) or closely spaced QDs (namely, "QD molecule") as building blocks for future quantum computation and quantum cryptography.[7–9] In this case, site-controlled low density QD structures are required to allow individual QD or QD molecule to be optically/electrically addressed. However, the achievement of site-controlled QDs or QD molecules has always presented a challenge due to the stochastic nature of self-assembled growth. Commonly, the fabrication of nanohole templates is an important technique for obtaining site-controlled quantum nanostructures based on the control of QD nucleation sites by the patterned nanoholes. Several approaches using artificial substrate process techniques, such as atomic force microscopy (AFM) tip oxide, scanning tunneling probe-assisted nanolithography, and electron beam lithography,[10–13] have been developed to obtain nanohole templates for growing ordered QDs or QD molecules. The great advantage of these methods is flexible control of the nanohole ordering. But these methods require complicated and expensive substrate processing instruments and also easily induce defects and chemical contamination. Recently, our group has begun to develop nanohole fabrication technique based on self-assembly in droplet epitaxy growth. By controlling the selective growth of GaAs during the crystallization of the Ga droplet, we obtained GaAs nanoholes of different shapes.[14–17] This method is simple, flexible, with no requirement for artificial substrate processing. In this letter, based on droplet epitaxy growth, we exploited a nanodrill technique to fabricate nanoholes on GaAs(100).

Droplet epitaxy was first proposed by Koguchi and Ishige[18] and Watanabe and Koguchi[19] with lattice-matched materials systems as an alternative approach to grow nanostructures. This growth technique has the flexibility to form versatile nanoholelike quantum structures and has shown promise as a method to achieve site-controlled QDs or QD molecules with low density and excellent optical properties.[15,16] In this research, all the samples were grown on a semi-insulating GaAs(100) surface by droplet epitaxy growth in a molecular beam epitaxy (MBE) chamber. In order to obtain nanoholes, we first grew sample A, using growth procedures similar to those described in Ref. 15. Following oxide desorption and growth of a 0.5 μm GaAs buffer layer at 600 °C, the substrate was cooled down to 500 °C. The arsenic (As) valve was fully closed before reaching the desired substrate temperature. Once the growth temperature was reached, gallium (Ga) flux equivalent to form 20 ML GaAs was supplied to the substrate surface to form Ga droplets. The sample was then annealed at 500 °C for 100 s under As flux with the valve 5% opened (corresponding to a beam equivalent pressure of $\sim 1.1 \times 10^{-6}$ Torr). Finally, sample A was quenched and taken out from the MBE chamber for analysis using AFM.

The resulting AFM image of sample A in Fig. 1(a) shows that the Ga droplets have fully crystallized after 100 s of annealing at 500 °C and nanohole structures are observed on the sample surface. A typical nanohole structure is shown in the inset of Fig. 1(a) and its cross-section profiles are given in Fig. 1(b) [the definitions of the width, the depth, and the lobe of the nanohole are shown in Fig. 1(b)]. The AFM image and the profile line both indicate that the holes have an average width of $s \approx 160$ nm, a depth of $d \approx 5.7$ nm, and a number density of ~ 3.3 μm^{-2}. Meanwhile, the nanoholes have an anisotropic lobe structure around the hole, which has an average height of $h \approx 9.1$ nm along the [01-1] direction and an average height of $h \approx 5.6$ nm along the [011] direction. Similar shaped nanohole structures have been observed previously for droplet epitaxy growth and the formation of the nanoholes was attributed to the selective growth of GaAs around the Ga droplet boundary during the crystallization of Ga droplets.[14,15] However, when we carefully analyze the depth distribution of the nanoholes, as shown by the histogram in Fig. 1(c), we found that there are some holes with a depth much larger than the total GaAs deposition of 20 ML ($\sim$5.7 nm) and some holes are even as deep at 12 nm. This indicates that, to a certain degree, the nanoholes are formed by etching into GaAs substrate. Clearly, these deep holes cannot be explained by the growth model referenced,[14,15] in which the nanoholes did not extend beyond the 20 ML of total GaAs deposition. Therefore there must be some differ-

[a]Author to whom correspondence should be addressed; FAX: 479 575 4580; electronic mail: liang@uark.edu

 © 2007 American Institute of Physics
Downloaded 03 May 2007 to 130.184.202.167. Redistribution subject to AIP license or copyright, see http://apl.aip.org/apl/copyright.jsp

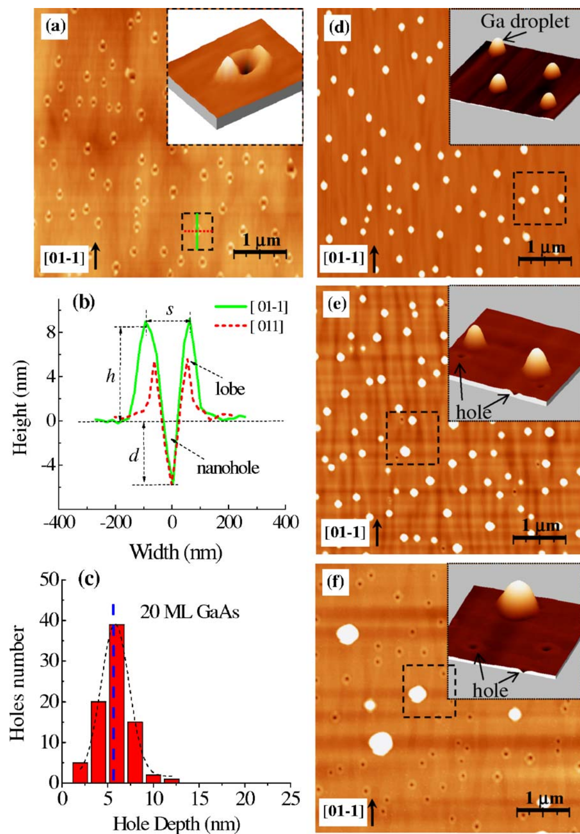

FIG. 1. (Color online) (a) $5\times 5\ \mu m^2$ AFM image of GaAs nanoholes formed on sample A surface. The inset, as is always the case in this letter, is the magnified AFM image showing the three-dimensional structure of a typical area given by the dashed line rectangle. (b) Line profiles of the exampled nanohole. (c) The histogram of nanohole depth distribution. (d) $5\times 5\ \mu m^2$ AFM image of sample B—taken out of the chamber immediately after 20 ML Ga deposition. (e) $5\times 5\ \mu m^2$ AFM image of sample C—taken out of the chamber after 2 min GI. (f) $5\times 5\ \mu m^2$ AFM image of sample D—taken out of the chamber after 10 min GI.

ent physical principles controlling the formation of nanoholes in our growth.

In order to obtain a more detailed picture, we grew three further samples (B, C, and D) to check the surface morphology evolution. Sample B was taken out of the chamber immediately after 20 ML Ga deposition. As shown by Fig. 1(d), the AFM image of sample B reveals that the deposited liquid Ga forms nanodroplets on the substrate surface, thereby minimizing the system's energy.[15] The Ga droplets randomly distribute on the substrate surface with an average lateral size of $\sim$150 nm, an average height of $\sim$45 nm, and a number density of $\sim 3.4\ \mu m^{-2}$. In Fig. 1(e), the AFM image of sample C shows the surface nanostructures that are transformed from the Ga droplets after 2 min of growth interruption (GI) with the As valve kept closed. The Ga droplets now show a reduced number density of $\sim 3.0\ \mu m^{-2}$, but the dimensions of the droplets increase to an average lateral size of $\sim$220 nm and an average height of $\sim$50 nm. The change in density and size is due to ripening of the droplets. The Ga droplets on the surface always have the tendency to merge together to reduce the system's energy. It is very interesting that we observed nanoholes appearing on the substrate surface. These holes had a lateral width of $s\approx 100$ nm, an average depth of $d\approx 9.9$ nm, and a number density of $\sim 0.18\ \mu m^{-2}$. The lobe of the nanoholes is anisotropic, which has an average height of $h\approx 3.0$ nm along the [01-1] direction and an average height of $h\approx 2.6$ nm along the [011] direction. We further increased the GI time to 10 min to produce sample D. As shown by Fig. 1(f), the droplets dramatically reduce in number density to $\sim 0.27\ \mu m^{-2}$ and increase in size to an average width of $\sim$450 nm and an average height of $\sim$107 nm. Remarkably, there were more nanoholes appearing on the surface. These holes had a number density of $\sim 3.3\ \mu m^{-2}$ and their dimensions increased to a lateral width of $s\approx 119$ nm and an average depth of $d\approx 12.5$ nm. The anisotropic lobe of the nanohole has an average height of $h\approx 4.1$ nm along the [01-1] direction and an average height of $h\approx 2.9$ nm along the [011] direction. The formation of GaAs droplet islands has been reported, but this is the first experimental observation of nanohole formation before the As was supplied to crystallize the Ga droplets. It is clear that these holes are not formed due to the crystallization of the Ga droplet. Meanwhile, the variation of the dimensions (depth, lateral size, and lobe height) of the nanoholes indicates that the GI process takes an important role in the formation of nanoholes.

Based on the above observations, we propose a simple model to describe the nanohole formation in our growth. First, in the experimental conditions without As ambience, the deposited Ga formed liquid nanodroplets in order to minimize the system's energy.[15,20] As the growth continued without As ambience, the Ga droplets on the substrate surface continued to ripen. They had the tendency to merge into bigger droplets to further minimize their energy. For this reason the Ga droplets kept reducing their number density and increasing their dimensions, as shown from Fig. 1(d) to Fig. 1(f) with lengthening GI time. Meanwhile, following the formation of Ga droplets, the interface between the droplet and the GaAs substrate became a Ga-rich area. It is well documented that, at a high temperature of 500 °C, GaAs is unstable under Ga-rich conditions and As desorption could occur.[21] So in the interface region the GaAs substrate will dissolve into Ga and As. As illustrated by Fig. 2(a), the As atoms may go through the Ga droplet, escaping into the vacuum chamber or they may diffuse to the boundary area of the Ga droplet and form GaAs again with Ga atoms from the droplet. This is probably the reason that GaAs lobes form around the nanoholes in Figs. 1(e) and 1(f) even before the As valve is opened. The remaining Ga atoms at the interface region after As desorption merge into the Ga droplet. As this process continues, there are more GaAs underneath the droplet dissolving, more Ga atoms from the GaAs substrate joining the Ga droplet, and more As atoms diffusing to the boundary region to form GaAs again. As shown by Figs. 2(b) and 2(c), the Ga droplet acted as a "nanodrill" etching into the GaAs substrate to give rise to nanoholes. The underlying physical principles for the nanodrill are totally different from previous reports of nanohole formation based on droplet epitaxy.[14,15]

Obviously, this nanodrill is strongly affected by the GI process. Before an As flux is supplied, the Ga droplet continues to act like a nanodrill etching into the GaAs substrate, forming nanoholes on the substrate. Evidently, nanoholes with larger number density and bigger dimensions were obtained as the GI time increased from 2 to10 min, as illustrated in Figs. 1(e) and 1(f). However, as soon as the As flux is supplied, the Ga droplet crystallization becomes the dominant growth mechanism since it is much faster than the nanodrill process. In fact, the formation of the nanoholes shown

Downloaded 03 May 2007 to 130.184.202.167. Redistribution subject to AIP license or copyright, see http://apl.aip.org/apl/copyright.jsp

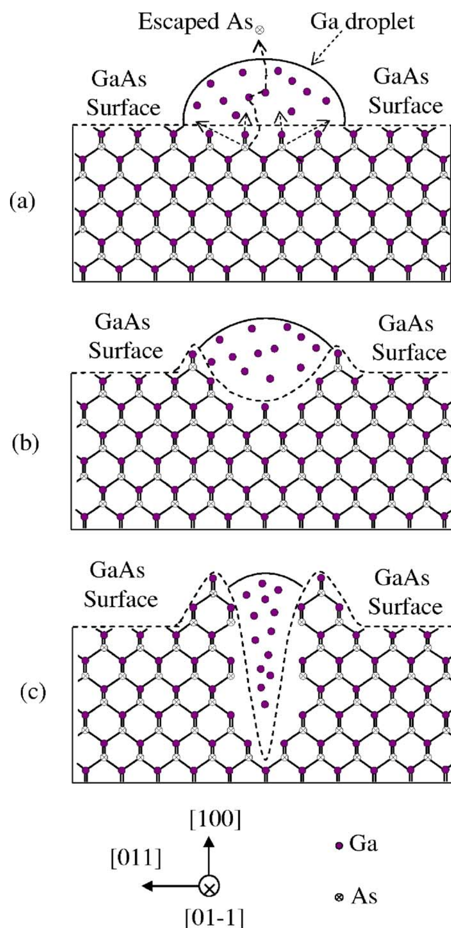

FIG. 2. (Color online) Schematic illustration of the proposed model for Ga nanodrill.

in Fig. 1(a) is a simultaneous combination of the Ga droplet nanodrill process, the Ga droplet ripening process, and the Ga droplet crystallization process. It can be expected that this combination can be tuned by the growth temperature, GI time, and annealing As pressure to obtain nanoholes with different shapes and depths. As an example, we finally grew sample E using the same growth conditions as sample A, except that after the droplets formed we kept the arsenic valve closed and inserted a step of 80 s GI at 500 °C to enhance the nanodrill effect. The resulting AFM for sample E is shown in Fig. 3(a) and the histogram of hole's depth is shown in Fig. 3(b). In this case, most of the nanoholes had a depth of more than 20 ML of GaAs deposition. The nanoholes have an average width of $s \approx 162$ nm, a depth of $h \approx 13.2$ nm, and a number density of $\sim 3.3\ \mu\mathrm{m}^{-2}$.

In conclusion, a self-assembled nanodrill technology based on droplet epitaxy growth has been developed to obtain nanoholes on GaAs(100) surface. Within this nanodrill technology, the gallium droplets act like "electrochemical drills" etching away the GaAs substrate to give rise to nanoholes that can penetrate the substrate to a depth greater than 10 nm. The driving force of the nanodrill is attributed to the As desorption underneath the Ga droplet at high growth temperatures and Ga-rich conditions. This nanodrill technology provides an easy and flexible method to fabricate nanohole template on GaAs (100) surface and has huge potential for developing quantum dots and quantum dot molecules for the quantum computation applications.

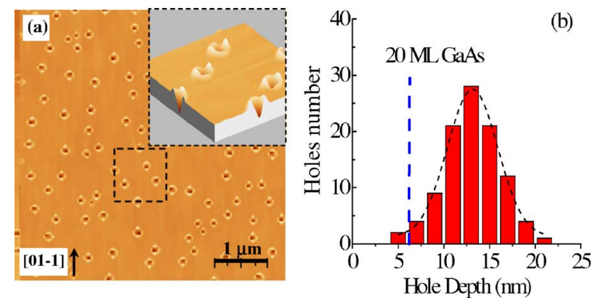

FIG. 3. (Color online) (a) $5 \times 5\ \mu\mathrm{m}^2$ AFM image of nanoholes formed on sample E with the inset showing the three-dimensional structure of a $1 \times 1\ \mu\mathrm{m}^2$ area given by the dashed line rectangle. (b) The histogram of nanohole depth distribution.

The authors acknowledge the financial support of the NSF (through Grant No. DMR-0520550).

[1]M. Bayer, O. Stern, P. Hawrylak, S. Fafard, and A. Forchel, Nature (London) **405**, 923 (2000).
[2]Z. Yuan, B. E. Kardynal, R. M. Stevenson, A. J. Shields, C. J. Lobo, K. Cooper, N. S. Beattie, D. A. Ritchie, and M. Pepper, Science **295**, 102 (2000).
[3]R. Schmidt, U. Scholz, M. Vitzethum, R. Fix, C. Metzner, P. Kailuweit, D. Reuter, A. Wieck, M. C. Hubner, S. Stufler, A. Zrenner, S. Malzer, and G. H. Dohler, Appl. Phys. Lett. **88**, 121115 (2006).
[4]K. G. Eyink, D. H. Tomich, J. J. Pitz, L. Grazulis, K. Mahalingam, and J. M. Shank, Appl. Phys. Lett. **88**, 163113 (2006).
[5]G. Fasching, F. F. Schrey, T. Roch, A. M. Andrews, W. Brezna, J. Smoliner, G. Strasser, and K. Unterrainer, Physica E (Amsterdam) **32**, 183 (2006).
[6]Z. L. Miao, Y. W. Zhang, S. J. Chua, Y. H. Chy, P. Chen, and S. Tripathy, Appl. Phys. Lett. **86**, 031914 (2005).
[7]J. R. Petta, A. C. Johnson, J. M. Taylor, E. A. Laird, A. Yacoby, M. D. Lukin, C. M. Marcus, M. P. Hanson, and A. C. Gossard, Science **309**, 2180 (2005).
[8]S. S. Li, J. B. Xia, J. L. Liu, F. H. Yang, Z. Ch. Niu, S. L. Feng, and H. Zh. Zheng, J. Appl. Phys. **90**, 6151 (2001).
[9]A. Rastelli, S. Stufler, A. Schliwa, R. Songmuang, C. Manzano, G. Costantini, K. Kern, A. Zrenner, D. Bimberg, and O. G. Schmidt, Phys. Rev. Lett. **92**, 166104 (2004).
[10]M. Vitzethum, R. Schmidt, P. Kiesel, P. Schafmeister, D. Reuter, A. D. Wieck, and G. H. Dohler, Physica E (Amsterdam) **13**, 143 (2002).
[11]J. S. Kim, M. Kawabe, and N. Koguchi, Appl. Phys. Lett. **88**, 072107 (2006).
[12]E. S. Moskalenko, F. K. Karlsson, V. T. Donchev, P. O. Holtz, B. Monemar, W. V. Schoenfeld, and P. M. Petroff, Nano Lett. **5**, 2117 (2005).
[13]S. Kiravittaya, R. Songmuang, A. Rastelli, H. Heidemeyer, and O. G. Schmidt, Nanoscale Research Letters **1**, 1 (2006).
[14]Z. M. Wang, K. Holmes, J. L. Shultz, and G. J. Salamo, Phys. Status Solidi A **202**, R85 (2005).
[15]Z. M. Wang, K. Holmes, Yu. I. Mazur, K. A. Ramsey, and G. J. Salamo, Nanoscale Research Letters **1**, 57 (2006).
[16]B. L. Liang, Z. M. Wang, J. H. Lee, K. A. Sablon, Yu. I. Mazur, and G. J. Salamo, Appl. Phys. Lett. **89**, 043113 (2006).
[17]J. H. Lee, Zh. M. Wang, N. W. Strom, Yu. I. Mazur, and G. J. Salmao, Appl. Phys. Lett. **89**, 202101 (2006).
[18]N. Koguchi and K. Ishige, Jpn. J. Appl. Phys. **32**, 2052 (1993).
[19]K. Watanabe, N. Koguchi, and Y. Gotoh, Jpn. J. Appl. Phys., Part 2 **39**, L79 (2000).
[20]Z. Gong, Z. C. Niu, S. S. Huang, Z. D. Fang, B. Q. Sun, and J. B. Xia, Appl. Phys. Lett. **87**, 093116 (2005).
[21]A. Y. Cho and J. R. Arthur, Prog. Solid State Chem. **10**, 157 (1975).

Downloaded 03 May 2007 to 130.184.202.167. Redistribution subject to AIP license or copyright, see http://apl.aip.org/apl/copyright.jsp